J Sol-Gel Sci Technol (2016) 79:279–294
DOI 10.1007/s10971-015-3882-2

ORIGINAL PAPER: FUNCTIONAL COATINGS, THIN FILMS AND MEMBRANES (INCLUDING DEPOSITION TECHNIQUES)

Structure–property tuning in hydrothermally stable sol–gel-processed hybrid organosilica molecular sieving membranes

J. E. ten Elshof[1] · **A. P. Dral**[1]

Received: 23 July 2015 / Accepted: 30 September 2015 / Published online: 27 October 2015

Abstract Supported microporous organosilica membranes made from bridged silsesquioxane precursors by an acid-catalyzed sol–gel process have demonstrated a remarkable hydrothermal stability in pervaporation and gas separation processes, making them the first generation of ceramic molecular sieving membranes with sufficient performance under industrially relevant conditions. The commercial availability of various α,ω-bis(trialkoxysilyl)alkane and 1,4-bis(trialkoxysilyl)benzene precursors facilitates the tailoring of membrane properties like pore size and surface chemistry via the choice of precursor(s) and process variables. Here, we describe the engineering of sols for making supported microporous thin films, discuss the thermal and hydrothermal stability of microporous organosilicas and give a short overview of the developments and applications of these membranes in liquid and gas separation processes since their first report in 2008.

Graphical Abstract

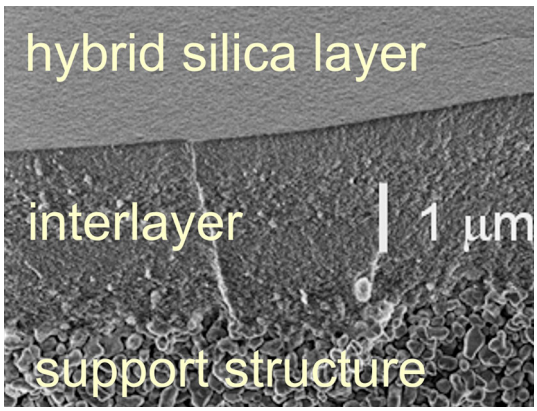

Keywords Microporous · Bridged silsesquioxane · Organically modified silica · Pore chemistry · Permselectivity · Separation

1 Introduction

Microporous ceramic membranes have been receiving considerable attention since the late 1980s because of their ability to separate gases and liquids on the molecular scale [1–3]. Very high gas separation selectivities have been reported for acid-catalyzed sol–gel-derived silica membranes, which are typically based on the use of tetraethyl orthosilicate (TEOS) as precursor [4]. According to the official IUPAC definition, "microporous" refers to pore diameters <2 nm, where the physical interaction between the transported molecule and the pore wall is significant, and interactions between transported molecules are much

✉ J. E. ten Elshof
j.e.tenelshof@utwente.nl

[1] MESA+ Institute for Nanotechnology, University of Twente, P.O. Box 217, 7500 AE Enschede, The Netherlands

less relevant than when the pore size would be larger. The molecular transport mechanism in the microporous size range is sometimes referred to as "single-file diffusion," because the pores are too narrow to allow parallel passage of two molecules.

Due to the high thermal stability of ceramic materials, microporous ceramic membranes offer an interesting route to high-temperature gas and liquid separation processes such as methane reforming, steam reforming and dehydration of organic solvents and bioethanol. Unfortunately, amorphous microporous silica is rather unstable at high temperatures in the presence of water, i.e., under hydrothermal conditions [5]. Even operating temperatures as low as 100 °C lead to performance loss and membrane failure within days or weeks of operation. The main reason for the poor stability of silica is the hydrolytic instability of the ≡Si–O–Si≡ bonds that can easily break upon reaction with water: ≡Si–O–Si≡ + H_2O → 2≡Si–OH, leading to dissolution of membrane material, pore widening and ultimately loss of membrane selectivity.

The hydrothermal stability was improved by introduction of methyl groups in the silica network structure, yielding so-called methylated silica membranes [5, 6]. It was thought that while the structure of the silica network still consists entirely of ≡Si–O–Si≡ bonds, the presence of terminal hydrophobic methyl groups shields these centers from water. Some improvement of stability was achieved, but still insufficient for use in industrial processes where water (vapor) is always present. Only the introduction of hydrolytically stable ≡Si–C_2H_4–Si≡ bonds in the network structure in 2008 resulted in a microporous silica-based membrane with good membrane separation properties for the removal of water from *n*-butanol, with long-term stability at the industrially relevant temperature of 150 °C [7], see Fig. 1.

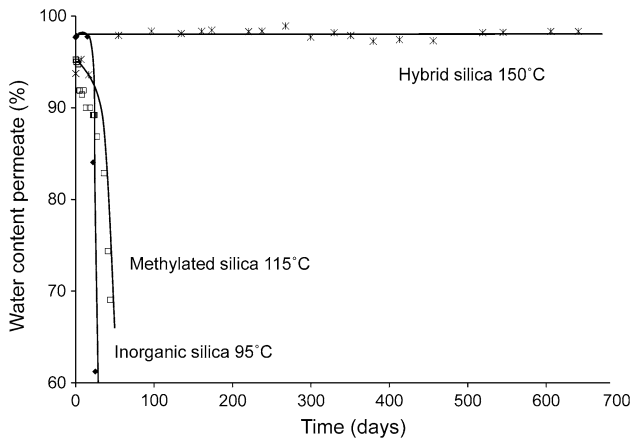

Fig. 1 Water content in permeate for a hybrid organosilica membrane operating continuously at 150 °C in pervaporation of 5 wt% water–95 wt% *n*-butanol. Selectivity is compared with methylated and inorganic silica membranes. Reproduced from Ref. [7] with permission from The Royal Society of Chemistry

The development of this so-called hybrid silica or hybrid organosilica membrane has led to renewed interest in molecular separations of gases and liquids under harsh conditions. Hybrid organosilica membranes are made by sol–gel processing using bridged silsesquioxanes $(OEt)_3Si–R–Si(OEt)_3$ similar to structure **1** in Fig. 2, where R is an organic bridging group. Hybrid organosilicas are suitable materials for molecular sieving applications because they can form pores with sizes ≪0.5 nm. Moreover, in contrast to other microporous membranes such as amorphous titania [8], they lack any tendency to crystallize, which would otherwise lead to larger grains and non-selective mesopores. The necessity to form a very thin film with a narrow pore size distribution and without any pores (defects) larger than a molecular diameter clearly shows the need to understand and control all stages of the film-forming sol–gel process in detail.

The present article presents a concise overview of the main developments and state of the art in hybrid organosilica membranes for molecular separations since their first report in 2008 [7], with some emphasis on the work done in our group at the University of Twente, in collaboration with the University of Amsterdam and the Energy Center of the Netherlands (ECN). The discussion is limited to "hybrid" organosilica membranes, i.e., 3D bonded networks containing ≡Si–O–Si≡ and ≡Si–R–Si≡ groups with homogeneous dispersion of both types of bonds on the atomic scale. For a review of the sol–gel processing of amorphous microporous silica and organically modified silica membranes, the reader is referred to other sources [9–11].

Bridged silsesquioxanes that have already been reported for hybrid organosilica membranes contain aliphatic or aromatic bridging groups [12–14]. The precursors referred to in this article are α,ω-bis(triethoxysilyl)-R compounds, where R is an alkylene $–C_nH_{2n}–$ (n = 1, 2, 3, 6, 8, or 10), ethenylene ($–C_2H_2–$), ethynylene (–C≡C–) or an arylene

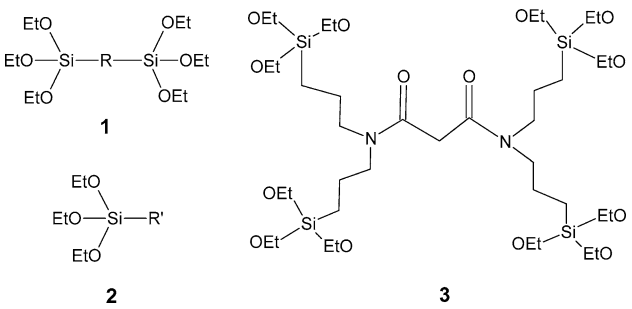

Fig. 2 Sol–gel precursors—**1**: bridged silsesquioxane precursor with bridging R group; **2**: silsesquioxane precursor with terminal R' group; **3**: *N*,*N*,*N*′,*N*′-tetrakis-(3-(triethoxysilyl)-propyl)-malonamide

like *p*-phenylene (–*p*-C_6H_4–) or di-*p*-phenylene (–*p*-C_6H_4–*p*-C_6H_4–). Co-condensation with other organically modified silicon alkoxides is also possible, typically by using triethoxy organosilanes such as structure **2** in Fig. 2, where R' can be a methyl, ethyl, propyl or other terminating organic group. In particular, the methylated precursor methyltriethoxysilane (MTES; R' = –CH_3) that was also used to make the first methylated silica membrane [15] is being referred to several times in this paper. Functionalization of the hybrid matrix by co-condensation of 1,2-bis(triethoxysilyl)ethane (BTESE) with an amine-functional silane precursor has also been reported [16]. Very recently, the use of more complex precursors has been reported, such as structure **3** in Fig. 2 [17] and a triazine-functional precursor [18]. In addition to membrane modification by organic bridging and pending end groups, selective doping with transition metal cations to alter the chemical environment within the hybrid organosilica matrix has also been investigated and is discussed below.

In the next section, the most important design rules for obtaining hybrid organosilica sols suitable for the formation of supported thin films without large defects are explained. Especially the relationship between the engineering of the sol and the final pore size and pore structure, and the evolution of nano- and microstructure in drying sol–gel thin films are discussed. In Sect. 3, the thermal and hydrothermal stability of hybrid organosilicas is discussed based on their molecular design. In Sect. 4, a short overview is given of the most important studies in which hybrid organosilica membranes have been employed for liquid and gas separation processes.

2 Sol–gel engineering of microporous hybrid organosilica membranes

The formation of a microporous membrane layer with size- or affinity-based molecular sieving properties from organically modified silicon alkoxide precursors requires the evolution of a condensed network with a narrow pore size distribution in the range of an individual molecule, i.e., 0.2–0.5 nm. Microporous silica-based membranes are usually made by a sol–gel process involving a dip, spin or flow coating step to form a thin film on an underlying mesoporous substrate (mesopores have a diameter of 2–50 nm according to IUPAC definition), followed by a thermal treatment. The microporous layer is 20–300 nm thick. The mesoporous substrate on which this layer rests consists of a γ-Al_2O_3 [7, 19, 20], anatase [21] or other mesoporous layer and has pore sizes of 3–10 nm. Since permselective silica membranes are very resistive to molecular transport, its thickness should be kept as low as possible to maximize the flux under a given concentration gradient. The mesoporous substrate acts merely as a low-roughness support layer on which a very thin smooth microporous film can be formed.

2.1 Sol–gel synthesis

In order to form a microporous film without mesopores, acid-catalyzed sol–gel processing is employed, typically with [Si] = 0.5–2 M and [H^+]/[Si] ratios around 0.1. The acid-catalyzed sol–gel process leads to branched oligomeric chains of condensed silicon alkoxide-derived monomer units as discussed in more detail below. Slightly branched polymeric sol particles are able to interpenetrate each other during the drying process, so that a relatively dense and homogeneous matrix can be formed, in which large pores are avoided that would typically develop when dense particles are packed (hard sphere packing). Since the microporous layer is made by coating onto a porous underlying substrate matrix, the sol size needs to be at least as large as the size of the pores of the underlying mesoporous substrate. Otherwise penetration of the sol would occur, leading to a resistive interface.

In early studies on hybrid organosilica membranes based on BTESE, it was attempted to avoid the formation of condensed bicyclic carbosiloxanes [7, 19]. Such oligomers have been reported to slow down or even inhibit gelation and may not become incorporated in a continuous network structure [22, 23]. To lower the statistical chance of forming inert cyclic oligomers, BTESE was mixed with MTES in a 1:1 molar ratio. Although MTES is known to hydrolyze considerably faster (1.2×10^{-3} OH/Si s^{-1} at 273 K) than TEOS (0.11×10^{-3} OH/Si s^{-1}) and BTESE (0.42×10^{-3} OH/Si s^{-1}), the rates and degrees of condensation under comparable reaction conditions were relatively similar, see Fig. 3 [24]. Hence, mixing of TEOS, MTES and BTESE precursors leads to a substantial degree

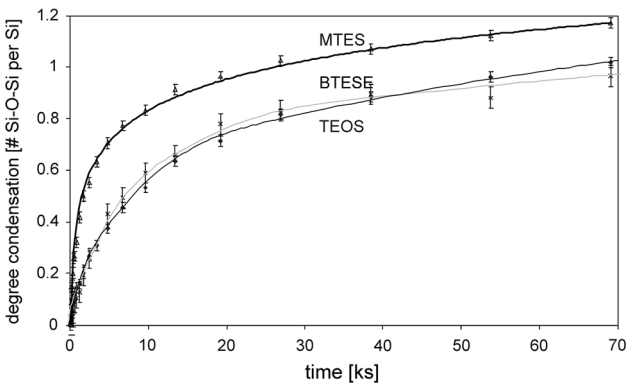

Fig. 3 Degree of condensation for three silicon alkoxides (TEOS, MTES and BTESE) measured at [Si] = 1.8 M, [H^+]/[Si] = 0.1 and [H_2O]/[Si] = 0.25 at 273 K. Reprinted from Ref. [24]

of co-condensation of dissimilar precursor types. In this way, the degree of condensation of BTESE into inert dimeric species can be minimized [19].

To optimize the degree of co-condensation further, the high silane reactivity toward hydrolysis can be moderated by employing water-lean conditions ($[H_2O]/[Si] = 0.5–2$) and low temperatures during mixing. To avoid a wide distribution of sizes in the sol, the hydrolysis is often carried out in two steps so that water-lean conditions are maintained throughout the process [24]. It is noted that in later studies hybrid organosilica membranes were mostly prepared from a single type of alkoxide precursor such as BTESE or bis(triethoxysilyl)methane (BTESM) [12, 25, 26], although condensation of monomers into relatively inert cyclic dimers that do not contribute to gel formation may have led to a decreased yield in these cases [22, 27].

BTESE/MTES sols with hydrodynamic diameters (=colloid size + solvation shell) of 2.2 nm as determined by dynamic light scattering (DLS) were reported to penetrate extensively into the underlying γ-Al_2O_3 substrate layer with 6-nm-wide pores upon dipcoating. Comparable sols with an average size of 4.9 nm yielded defect-free membranes [19], but sols with an average hydrodynamic diameter of 13 nm formed thick films with visible macroscopic cracks after drying. High-throughput screening approaches have been employed to optimize the colloid size of various bridged precursors with methylene, ethylene, *p*-phenylene and di-*p*-phenylene bridging groups [28]. Hydrolysis ratio, acid ratio and reaction temperature were varied systematically. Under comparable synthesis conditions, BTESE and BTESM sols had comparable sizes (4–7 nm); the sols from the phenylene bridged precursor were smaller (<2.5 nm), while the di-phenylene bridged ones grew considerably larger (>20 nm). The variation in reactivity is mainly due to differences in the electron donating character of the alkylene and phenylene bridging groups.

2.2 Sol structure evolution monitored by in situ SAXS

Gradual bond formation during sol growth favors the development of a branched polymeric structure. Such sol particles can be considered as entities with a dimensionality that is larger than that of an unbranched one-dimensional chain (where mass is proportional to size), but smaller than that of a three-dimensional dense sphere (where mass is proportional to the third power of the size). For one- to three-dimensional objects, the relationship between mass m, radius of gyration R_g and dimensionality D_i can be generalized as

$$m \sim (R_g)^{D_i}$$

The gyration radius can be obtained from small-angle X-ray scattering (SAXS) experiments on sols using the universal relationship [29]

$$\lim_{q \to 0} I(q) \sim \exp\left(-R_g^2 q^2/3\right)$$

Here, $I(q)$ is the scattering intensity as a function of scattering vector q (nm^{-1}). Acid-catalyzed silica sols suitable for membrane formation usually have a radius of gyration $R_g \ll 10$ nm.

The parameter D_i, also termed the fractal dimension or dimensionality, can also be obtained from SAXS data. Essentially, D_i is a measure of the internal structure of a sol particle, e.g., it quantifies the degree of branchedness. In a limited q-range, the SAXS curves of silica-based sols show a linear relationship between log I and log q [29], i.e.,

$$I(q) \sim q^{D_i}$$

Larger values of D_i refer to more highly branched sols. Previous research on TEOS-based polymeric silica sols in the 1990s showed that defect-free microporous films are formed when $D_i = 1.2–1.5$ [30], although we have also obtained good results when D_i was slightly larger, i.e., 1.5–1.6. When D_i is too small, interpenetration of sol particles cannot occur, while penetration of the sol into the underlying support may occur easily. On the other hand, interpenetration of sol particles becomes impossible when $D_i \gg 1.6$ because a too high intraparticle density would prevent their centers of mass to approach each other enough.

The dominant growth mechanism under preparation conditions typical for sols for microporous membranes is diffusion-limited cluster aggregation (DLCA), which has been shown to result in structures with an ultimate D_i of 1.8–1.9 when the reaction time is long enough [30–32]. In DLCA, the approach of particles is governed by Brownian transport while the reaction rate is much higher than the rate of diffusion. A SAXS study on sols with $–CH_2–$, $–C_2H_4–$, $–C_8H_{16}–$, $–p\text{-}C_6H_4–$ and $–p\text{-}C_6H_4–p\text{-}C_6H_4–$ bridging groups showed that although the reactivity of the precursors varied, the values of D_i were similar ($D_i = 1.50–1.60$) when the radii of gyration were similar ($R_g = 1.5–2.3$ nm; hydrodynamic diameter 6 nm) [12]. Defect-free membranes with molecular sieving properties could be formed from all five sols.

The gelation of BTESE sols with hydrodynamic diameters of 5–6 nm was studied using time-resolved SAXS [33]. Ethanolic sols with $[H_2O]/[Si] = 1$, $[Si] = 0.9$ M and acid ratio $[H^+]/[Si] = 0.01$, 0.10 or 1.0 and an initial value D_i of 1.2 all grew to an ultimate value of $\sim$1.87, irrespective of $[H^+]/[Si]$, see Fig. 4. In contrast, when the same sols were applied as thin films and their structural evolution during film drying (solvent evaporation) at room temperature was monitored [33], the evolution of structure varied strongly

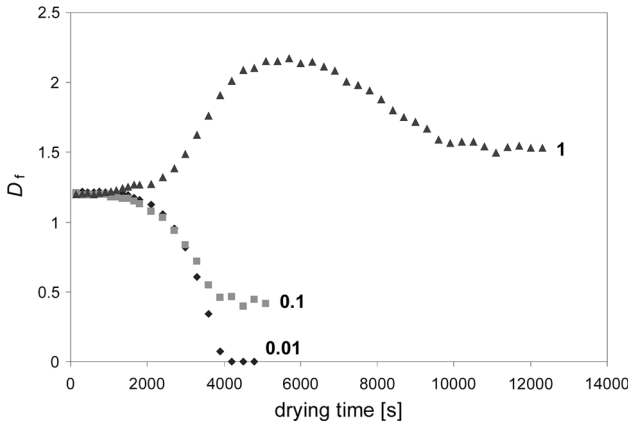

Fig. 4 Time-dependent evolution of D_i during drying at room temperature of BTESE-based sols with H^+:Si molar ratios of 0.01, 0.1 and 1. Adapted from Ref. [33], with permission from Elsevier

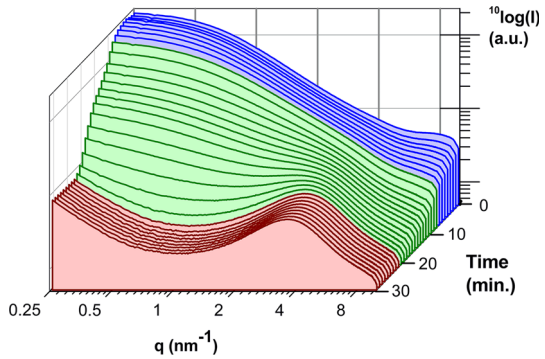

Fig. 5 Evolution of SAXS curves during the drying of a thin film of NPE–BTESE at 60 °C. Colors are a guide to the eye and indicate the three stages of drying as discussed in the text. Reprinted from Ref. [34] with permission from Elsevier (Color figure online)

from one sample to the other. For the sample with $[H^+]/[Si] = 0.01$, D_i decreased to an ultimate value of zero, suggesting the formation of a homogeneous film without pores that are visible with SAXS ($\sim$0.5 nm or larger). The film with $[H^+]/[Si] = 0.1$ exhibited a smaller decrease in scattering intensity, and D_i reached a final value of $\sim$0.4 in the as-dried film. This suggests a film with a final "fractal-like" pore structure. The film with $[H^+]/[Si] = 1$ showed more complex behavior during drying, but the ultimate D_i value was $\sim$1.5. The data suggest a slow densification process, but less than in the other two cases. Thermal treatment of similarly dried powders at 523 K in N_2 atmosphere resulted in BET surface areas of 0, 632 and 970 m^2/g, respectively [33], and pore sizes $d_p < 0.30$ (N_2 size), 1.5 and 2.7 nm, respectively.

In other words, the presence of H^+ is necessary to construct and/or maintain a porous network structure in the drying film during the solvent evaporation process. Capillary forces and compressive stresses during drying and film shrinkage promote the densification of the hybrid organosilica network into a dense structure with small or virtually no pores. At high acid concentration, these forces seem to be counteracted. Possibly the network is strengthened by ongoing condensation reactions due to the H^+ concentration and by the positive charge on the polymeric colloidal network. The pore structure can be adapted by adjustment of the acid-to-Si ratio before the onset of physical drying, while the rheological properties needed for film coating are retained. This study clearly demonstrates the importance of the H^+ concentration to tailor the pore size of a hybrid organosilica membrane.

2.3 Incorporation of transition metal cations

While the co-condensation of (bridged) silsesquioxanes is relatively simple owing to the roughly similar reactivity of the precursors, the incorporation of transition metal ions on atomic scale to change the local chemistry and pore wall polarity is complicated. Transition metal alkoxides are much more reactive and will thus condense on much smaller time scales than silicon precursors. A well-known strategy in sol–gel processing to disperse a transition metal into a silicon alkoxide based matrix is a two-step sol–gel reaction involving prehydrolysis of the silicon alkoxide precursor prior to addition of the transition metal alkoxide in the second step.

A good case study is the preparation of Nb-doped BTESE films (Nb:Si = 1:4) studied by time-resolved SAXS. Mixing $Nb(OEt)_5$ (NPE) into a prehydrolyzed acidic BTESE sol in ethanol at 298–333 K was shown to lead to NbO_x clusters within the first 10 s of reaction [34, 35]. The presence or absence of preydrolyzed BTESE has a negligible influence on the size of these clusters. However, their subsequent growth and agglomeration is suppressed by the presence of BTESE [35], because the niobia particles/clusters become encapsulated by BTESE-derived moieties.

The time-resolved SAXS curves of a drying thin film of premixed NPE-BTESE are shown in Fig. 5 [34]. Three main stages can be distinguished in the film drying process, which are indicated by different colors. In the initial stage (blue), the SAXS curves decrease in intensity, but remain unchanged in shape except at high q. The intensity decrease is caused by loss of scattering mass from the film (solvent evaporation); the pronounced decrease at high q suggests that the smallest entities are disappearing from the solution. The region with constant slope at $q > 1.5$ nm^{-1} is suggestive of slightly branched isolated sol particles. The flattened curve at $q < 1.5$ nm^{-1} indicates the limited size of the sol particles ($\sim$3–4 nm). In the second stage (green), ethanol that initially surrounded the isolated sol particles has been replaced by other sol

particles. The low electron density contrast between sol particles and surroundings leads to a low scattering intensity in some regions. The phase inversion process solid-in-solvent to solvent-in-solid occurs in this stage. The relatively constant intensity at intermediate length scales ($q \approx 1$ nm^{-1}, i.e., $\sim$6 nm in real space, the typical dimension of a sol particle) in the third phase (red) indicates that the phase inversion had already occurred there and that the film is homogeneous and visually dry. The correlation peak at $q = 4$ nm^{-1} is due to NbO_x clusters in the BTESE matrix. The fact that the correlation peak is rather pronounced shows that the clusters are of approximately the same size and that they are located at more or less similar distances from each other in the matrix, i.e., homogeneously dispersed on a length scale of nanometers. The NbO_x clusters have a radius of 0.4 nm irrespective of prior reflux conditions and are spaced at average distances of 1.6 nm [34]. Hence, this route yields only a limited number of heterolinkages Nb–O–Si in the final network structure, as was also confirmed by a relatively large O-Nb_3 signal in ^{17}O NMR [36]. This indicates a BTESE-derived matrix containing mainly phase-segregated NbO_x domains and a low concentration of atomically dispersed Nb centers.

An alternative strategy to reduce the reactivity of metal alkoxides is to form complexes with strongly coordinating ligands prior to their reaction with silicon-based precursors. When 2-methoxyethanol and acetylacetone were employed to reduce the reactivity of NPE in BTESE, it was found that acetylacetone led to the formation of a large concentration of heterolinkages Si–O–Nb in the final material (Nb:Si = 1:4) [36]. The distribution of oxygen among Si–O–Si, Si–O–Nb and Nb–O–Nb was close to a statistical distribution, indicating that Nb was atomically dispersed in the BTESE matrix in this case. 2-Methoxyethanol only coordinated with a limited Nb^{5+} fraction unless all EtOH solvent was removed by evaporation, and was rather ineffective as stabilizing ligand.

A new strategy to incorporate and distribute a high concentration of arbitrary transition metal centers in a hybrid organosilica matrix was recently demonstrated by Besselink et al. [17]. Using a new malonamide-functional precursor with four Si atoms and 12 reactive ethoxy groups (see Fig. 2), a microporous membrane material was synthesized that contained a high concentration of metal ion-coordinating groups. Ni^{2+} and Ce^{4+} were successfully dispersed in this membrane matrix, but other transition metals are equally well possible. Although a fraction of these metal ions redistributed into small nanosized grains of CeO_2 (<5 nm) and Ni_2O_3 (<15 nm), these membranes exhibited higher gas separation selectivity than conventional BTESE membranes, as discussed below [17].

3 Thermal and hydrothermal stability

Silica-based membranes undergo thermal treatment prior to their operation to consolidate the microporous network. However, the introduction of organic groups in the glass matrix significantly affects its stability at elevated temperatures, and this must be considered when deciding on consolidation procedures and high-temperature applications of hybrid organosilica membranes. The organic groups are incorporated in the silica network on a molecular level, and this makes them more stable than analogous pure organics, but they cannot withstand the same temperatures as fully inorganic silica. For example, the methyl groups in methylated silica are reported stable up to 450–550 °C under inert atmosphere [19, 37–40] and up to 350–400 °C in the presence of oxygen [38, 40]. Placing organic groups in bridged configuration improves their thermal stability; methylene groups are reported stable up to 650 °C under inert atmosphere [41]. The reported upper temperature limits for bridging ethylene groups vary significantly under inert atmosphere, from 250 to 500 °C [19, 42–45], and are 200–300 °C in air [19, 23, 42]. Bridging phenylene groups can withstand 450 °C under nitrogen or air [46]. However, it is important to realize that the onset of thermal degradation may vary for different microstructures. Thermal degradation can be hindered by decreasing micropore size because this reduces the internal supply of oxygen and removal of degradation products. Furthermore, tight encapsulation of organic groups within the thermally stable silica network may also suppress decomposition reactions.

As discussed above, the value of hybrid organosilica materials as compared to pure silica in membrane technology originates from their hydrothermal stability. The introduction of organic bridges between silicon atoms impressively reduces the net effect of water on the overall network, despite the fact that the backbone still mostly consists of water-sensitive siloxane bonds. It is important to realize that classification of hydrothermal stability for membranes is generally based on their ability to maintain separation performance under hydrothermal conditions. This does not necessarily mean that water causes no change to the material at all; siloxane bonds are by nature susceptible to rehydrolysis and they may still be attacked by water. Glass will never become truly static. Thus, here we define the hydrothermal stability of hybrid organosilica materials as the absence of monomeric dissolution accompanied by preserved overall performance. Nevertheless, chemical and structural changes can and do still occur [47–49].

A first feature of hybrid organosilicas that is often brought up as an origin of their hydrothermal stability is the

hydrophobicity or nonpolarity introduced by the organic groups [19, 49–51]. Hydrophobic segments can reduce the overall amount of water entering the network and shield adjacent siloxane bonds, which makes it more difficult for water molecules to hydrolyze them. However, the effective hydrophobicity of organosilicas strongly depends on the molecular arrangement within the network. Organic groups that are directed toward the (internal) surface can act as a hydrophobic barrier that, in the extreme case, may completely prohibit water from entering the network underneath the surface. This would then yield maximum resistance against hydrolysis. Such effective hydrothermal stability cannot be classified as an intrinsic material property if it does not hold for other possible network organizations as well, but these molecular arrangements are at least in part dictated by the molecular design of the organosilica monomer. Monomers that are most likely to form hydrophobic surfaces are the ones with terminating organic groups [37, 40, 52–61] or with long and flexible organic bridges [53, 62]. Short or rigid bridges such as ethylene and *p*-phenylene do not have the length and spatial freedom to "step out" to the surface and completely shield the underlying siloxane bonds; thus, these materials keep on having a significant affinity for water [47, 48, 62–64]. Furthermore, when these materials are used for water-permeable microporous membranes, their networks explicitly require a significant degree of hydrophilicity. Their selective permeability for water proves significant interaction between silanol or siloxane segments and water and thus rules out hydrophobic shielding as main origin of hydrothermal stability. In addition, the observed hydrothermal instability of bridged organosilicas in water at basic pH [19, 33] confirms that the siloxane bonds are indeed accessible to aqueous species.

A second aspect that has been brought forward as possible origin of high hydrothermal stability is the increased connectivity of a monomer with the surrounding network when two silicon atoms are linked together by an organic bridge [19, 65]. The fourfold connectivity of pure silica monomers is increased to sixfold for organically bridged monomers. The chance that all siloxane bonds of a monomer unit are hydrolyzed and the monomer dissolves, decreases exponentially with increasing connectivity. This implies a drastic improvement of the hydrothermal stability by switching from terminating to bridging organic groups, as is indeed observed for microporous membranes with either terminating methyl or bridging ethylene groups [19]. However, to the best of our knowledge, the effect of monomer connectivity on hydrothermal stability has not been systematically studied. In addition to the number of siloxane bonds per monomer unit, the monomer size and mass may also play an important role via its diffusivity. This determines the actual displacement of a monomer once it has been fully disconnected from the surrounding network. Furthermore, apart from the theoretically possible network connectivity, the actual degree of condensation is also relevant. Full condensation is generally not reached for organosilica materials prepared via acid-catalyzed synthesis. A higher degree of condensation has been reported to increase the hydrothermal stability of pure silica mesoporous structures [66], but separating the increased condensation degree as such from other accompanying network reorganization effects like a change in empty space and bond strain is difficult.

A third property of hybrid organosilicas that has been put forward as contributing to hydrothermal stability is their structural flexibility [7, 19]. Siloxane bonds are more sensitive to hydrolysis when they are strained, but the organic segments can make the network less rigid and enable relaxation of stresses from drying, shrinkage and non-optimal network configurations. The overall flexibility scales with the length and flexibility of the bridge, though for larger organic groups the reduced overall connectivity may become a problem. Furthermore, the effective flexibility of a material is also related to the presence of empty volume within the network. Organic bridges act as spacers and can increase the microporosity. These microporous materials may be pictured as polymer-like networks with well-connected unoccupied volume rather than a bulk phase with discrete pores, but either way the empty space facilitates internal movement of the network toward a more relaxed state. With bridges that are too flexible or too bulky, empty spaces will collapse or get filled. The effects of flexibility and empty volume on hydrothermal stability have not been studied systematically. Nevertheless, an example of a bridging group that enhances microporosity and shows good performance over a range of mechanical properties is ethylene. The higher flexibility of ethylene-bridged silica as compared to pure silica allows fabrication of films with a thickness over 1 μm without crack formation during drying [67]. Its adhesive and cohesive fracture resistance is considerably higher than for carbon-doped silica in a non-bridged configuration [68], and it maintains a high Young's modulus at high porosities [68]. Theoretical models have been developed to predict elastic and fracture properties for other organosilica precursors [69].

Considering some intrinsic aspects of silica and water from a more fundamental molecular point of view may help to understand their interactions. Silica and water show many similarities as a substance. Both can be described as networks of corner-sharing tetrahedrons. In silica, silicon is semicovalently bonded to four oxygen atoms, where the Si–O bond has about 51 % ionic character and 55 % double-bond character [70, 71]. In water, oxygen is connected to four hydrogen atoms by covalent and hydrogen bonds. Silica and water have a range of analogous

crystalline phases [72] and share peculiar physical properties such as having density maxima in the liquid state [73] and having phases wherein viscosity decreases upon compression [74]. Also nanoclusters of water and silica show similar energetics and topologies [72], which is intriguing considering the extremely large surface-to-volume ratio of nanoclusters and the distinct ways in which water and silica cope with surface terminations. However, what may be the most important aspect in perspective of hydrothermal stability is that both water and silica form networks with an impressive structural freedom. Water has the abundance of hydrogen bonds that drive water molecules to interact with their environment and form (liquid) networks, but are also weak enough to be broken easily and allow continuous reorganization. Silica has an impressive structural freedom originating from the flexibility of the Si–O–Si bond angle. This angle can vary roughly between 134° and 180° [75], allowing the four-coordinated silicon tetrahedra to tilt and realign in many different ways. Such structural freedom also allows variations in packing density and the incorporation of empty spaces without compromising structural integrity. Furthermore, both water and silica can easily enter (transition) states with an excess or shortage of electrons on any of the atoms. All these parallels in molecular bases and abilities make silica and water fascinatingly suitable to play around in each other's network and create new configurations. The incorporation of organic segments in silica shifts the balance of these interactions, but cannot eliminate the dynamic nature of glassy networks. Hybrid organosilicas remain sensitive to internal reorganizations, via ongoing hydrolysis and condensation as well as via structural relaxation without breaking bonds. Though the mechanisms involved in these reorganizations remain unclear to date, occurrence over long periods of time is also relevant for membrane applications because it may affect the internal micropore structure of these materials.

4 Molecular sieving membranes

The three most important properties of a molecular sieving membrane are: (1) its semipermeable nature, i.e., its ability to be highly permeable for part of the species of a mixture of gases or liquids and serve as a barrier for the others; (2) the flux of the preferentially transported species through the membrane; and (3) the chemical and thermal stability of the membrane under operating conditions over a long period of time. The envisaged applications of hybrid organosilica membranes, namely industrial gas and liquid separations at high temperatures and under harsh chemical conditions, require high thermal and chemical stability in the presence of water over periods of years.

The principal parameter, membrane selectivity, defines whether a material can serve at all as a semipermeable barrier for a given separation. Membrane selectivity depends on variations in the abilities of species to travel through a membrane matrix. These abilities are expressed in terms of permeability P_i of a species i, which is proportional to the concentration c_i and mobility b_i, i.e., $P_i \sim b_i c_i$. For two given gases i and j, the ideal permselectivity $S_{i,j}$ of a membrane is defined as P_i/P_j. This value would have practical meaning if the respective fluxes would not be interfering with each other. For real processes, a separation factor α is defined to express the efficiency of the process, for example in terms of the ratio of ratios of concentrations of species i and j in a binary mixture at the feed (high pressure) and permeate (low pressure) side of the membrane, i.e.,

$$\alpha_{i,j} = \frac{(y_i/y_j)}{(x_i/x_j)}$$

where x and y are the concentrations of components i and j at the feed and permeate side, respectively. The permeability also determines the flux j_i, as it is a proportionality constant between flux and applied driving force (pressure or concentration difference) across a membrane,

$$j_i \sim -P_i \nabla c_i$$

Here, ∇c_i refers to the concentration gradient of species i. Earlier work on TEOS-derived microporous membranes showed that the dominant factor that determines the permeability of a species is the pore size of the membrane [4, 15, 76]. Smaller molecules can travel faster than larger ones. In these cases, the membrane permselectivity is primarily determined by the width of the pore size distribution. Ideally, the preferentially permeating species is just a fraction smaller than the average pore size, whereas no larger pores are present that allow permeation of the other (larger) non-preferred species.

4.1 Pervaporation

TEOS-derived silica is very permeable to small species with a kinetic diameter <0.3 nm like H_2, He and H_2O and impermeable to large gases like SF_6 (0.55 nm) and large organic molecules such as ethanol and *n*-butanol (>0.4 nm) [77]. The first reports demonstrating that hybrid organosilica membranes also have molecular sieving properties were published in 2008 [7, 19]. The first hybrid organosilica membrane was made from a 50:50 molar mixture of BTESE and MTES precursors, and it showed very good performance in the pervaporation dehydration of a 5/95 wt/wt water/*n*-butanol mixture at a temperature of 150 °C for more than a year, see Fig. 1. Appreciable water fluxes >10 kg m^{-2} h^{-1}

and a separation factor $\alpha_{H2O,BuOH} = 930$ were measured. It was the first generation of microporous ceramic membranes with a performance that may enable large-scale industrial application. TEOS-derived silica and methylated silica (MTES–TEOS) membranes would have degraded within hours under such conditions due to poor hydrothermal stability ($\equiv Si–O–Si\equiv + H_2O \rightarrow 2\equiv Si–OH$). The selectivity can be explained by considering adsorption data of unsupported BTESE–MTES powder made via the same sol–gel synthesis route. The powder was found to have a pore size larger than 0.24 nm (molecular size of C_2H_2), but smaller than 0.30 nm (size of adsorbed N_2), since it allowed substantial adsorption of C_2H_2 (1340 m^2/g), but no N_2 adsorption. In comparison, MTES-derived methylated silica with the same CH_x:Si ratio shows some adsorption of N_2 (12 m^2/g), as does microporous silica (33 m^2/g). On the other hand, their adsorption capacities for C_2H_2 were lower (211 and 261 m^2/g, respectively). These data suggest that the average pore size of BTESE–MTES hybrid organosilica is smaller than that of MTES- and TEOS-derived silica. Hence, at the same organic fraction as in BTESE, the pore size distribution of BTESE–MTES is narrower, and the adsorption capability for very small molecules (<0.3 nm) is larger.

In a follow-up study in the same year the first purely BTESE-based hybrid organosilica membrane was reported [65]. In view of the fact that its average pore size is larger (C_2H_2 adsorption 514–546 m^2/g; N_2 adsorption 131–311 m^2/g), the corresponding membrane was a priori expected to be less selective. In contrast, the separation factor in water/*n*-butanol pervaporation was higher than that of BTESE–MTES ($\alpha_{H_2O/BuOH} = 360–2700$ for BTESE versus $\alpha_{H_2O/BuOH} = 225$ for BTESE–MTES). These seemingly conflicting results show that not only pore size, but also factors like pore connectivity and physicochemical interactions between permeating species and the membrane matrix are important to consider. Even higher water fluxes and higher separation factors are obtained when the $–C_2H_4–$ bridge (BTESE) is replaced by $–CH_2–$ (BTESM) [25, 28]. The pore size of this system is between that of BTESE and BTESE–MTES [25]. Unlike BTESE and BTESE–MTES with a CH_x:Si ratio of 1, the CH_x:Si ratio of BTESM is only 0.5. Hence, the BTESM membrane has a more hydrophilic character than the ones discussed so far. The high water flux is likely at least partly due to the hydrophilic nature of the membrane. However, BTESM also showed a remarkable ability to separate water from lower alcohols, including the notoriously difficult molecular separation methanol–water [25, 77]. Using a 5:95 wt/wt water–methanol mixture at the feed side, a permeate stream containing 55:45 wt/wt water–methanol was accomplished ($\alpha_{H_2O/MeOH} = 23$), see Fig. 6. While such a selectivity may seem low in comparison with separation factors >1000 reported for water/*n*-butanol [78, 79], it should be taken into account that methanol and water are very similar in size and comparable in their polarity and hydrogen bonding capability. Not many membranes can separate this mixture effectively under high flux conditions. In comparison, BTESE–MTES and BTESE show no appreciable selectivity for methanol–water, and BTESE–MTES only has low selectivity for ethanol–water ($\alpha_{H_2O/EtOH} = 15$) [28]. BTESM has separation factors >150 for ethanol, *i*-propanol and *n*-butanol and shows higher water fluxes under otherwise similar conditions [28].

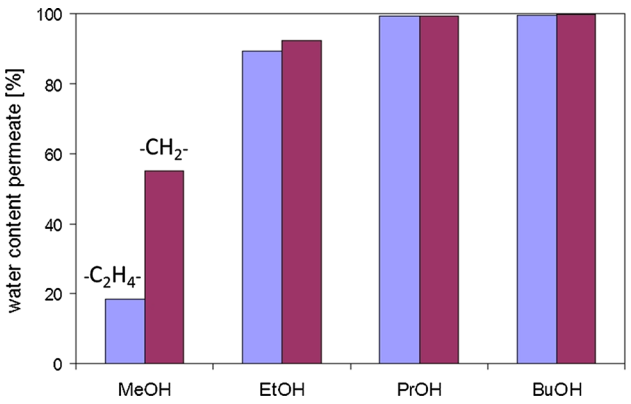

Fig. 6 Separation selectivity of BTESE ($–C_2H_4–$) and BTESM ($–CH_2–$) membranes in the pervaporation dehydration of 95/5 wt% alcohol/water feed mixtures at temperatures approximately 5 °C below the boiling point of the respective alcohol. Selectivity is expressed in terms of the weight fraction of water (wt%) in the permeate stream. Data were taken from Ref. [25]

Bridged silsesquioxane precursors with a high CH_x:Si ratio tend to have a longer bridge between the Si centers and are thus expected to yield membranes with a larger average pore size, although there is a limit to this effect especially for long flexible bridges. Of course, in addition to size selection the mobility of molecules in a microporous membrane matrix may also be influenced by polar and/or van der Waals interactions with the pore wall. Combinations of different precursors might allow the formation of microporous membranes with small pore size and hydrophobic character, but this is still a largely unexplored area of research. A water/*n*-butanol pervaporation study on hybrid organosilica membranes made from precursors with $–C_nH_{2n}–$ ($n = 1, 2, 8$) and $–(p\text{-}C_6H_4)_m–$ ($m = 1, 2$) bridges showed that the *n*-butanol flux was larger for the systems with $n = 8$ and $m = 2$ [12], while the water flux remained relatively constant. It suggests that while the permeability of less hydrophilic fluids like *n*-butanol is promoted by a higher CH_x:Si ratio, the accompanying enlargement of the pore size seems to be playing an equally significant role. Otherwise a high butanol flux would also have been expected for the system with $m = 1$, while the permeability of water should have been smaller for $n = 8$ and $m = 2$.

The influence of the hydrophobic character of the membrane was more pronounced in a study in which BTESE was mixed in a 1:1 molar ratio with a series of organosilicon precursors with terminal alkyl groups $(OEt)_3Si–C_xH_{2x+1}$ ($x = 1$, 2, 3, 6, or 10) [13]. A gradually increasing separation factor for *n*-butanol from a 95/5 wt/wt *n*-butanol/water mixture at 95 °C was observed when the terminal chain length (x) was increased, with an appreciable $\alpha_{BuOH/H_2O} = 14$ for $x = 10$, see Fig. 7 [13]. The permeability of water decreased gradually with increasing value of x. Aromatic bridges like *p*-phenylene and di-*p*-phenylene bridges (CH_x:Si = 6, 12) seem to be less effective in promoting the flux of *n*-butanol compared with alkyl bridges with similar CH_x:Si ratios [12].

4.2 Gas separation

While dehydration pervaporation seems to be a promising area of application of molecular sieving membranes, another class of separations for which microporous molecular sieving membranes are very suitable candidates is gas separations [50]. The obvious difference with separations in the liquid phase is the much smaller concentration of the feed stream, which is usually counteracted by application of high gas pressure at the feed side, i.e., 30–70 bar is common in the process industry. Industrially relevant gases include H_2, CO_2, CH_4 and CO, but also various hydrocarbons. The size differences between gas molecules are usually smaller than between molecules in the liquid phase. Moreover, the interaction between pore wall and gas molecule is usually less intensive, partly because hydrogen bonding is absent, and partly because gases like H_2, CH_4 and even CO are spherical and nonpolar so that they do not interact strongly with the pore wall [61]. Hence, the difference between the molecular sizes and the size of the pore is often the main factor determining gas separation selectivity. Since the molecular sizes of the abovementioned gases differ by less than 0.1 nm (H_2 0.29 nm; CO_2 0.33; N_2 0.36; CO 0.37; CH_4 0.38 nm), a very sharp pore size cutoff between the targeted molecule and all larger components of the mixture is required to obtain highly gas-selective membranes. Very high separation factors $H_2/N_2 > 4000$ have been reported for silica in the 1990s [4], but the permselectivity values are much lower for MTES-derived methylated silica [15]. The gas separation selectivity of hybrid organosilica membranes is also rather moderate [28, 50]. The low intrinsic permselectivity has been ascribed to the relatively open pore structure of $–C_2H_4–$ and $–C_2H_2–$ bridged silicas [42, 64], and that hypothesis is supported by molecular dynamics simulations of the pore size distribution of BTESE hybrid organosilica and silica [80, 81], see Fig. 8. There is a small, but considerable fraction of pores >0.4 nm that limits the separation of hydrogen from other larger industrial molecules and that is not present in silica.

Longer bridge lengths [12] and stiffer bridges [14] lead to larger pores and therefore to lower permselectivities, although long flexible chains such as $–C_8H_{16}–$ appear to collapse, leading to loss of permeability. On the other hand, BTESM-derived membranes with permselectivities of 15–21 for H_2/N_2 and 7–9 for H_2/CH_4 [28] perform only marginally better than BTESE-derived membranes in H_2 separation even though their bridge length is shorter. They show higher permselectivity in the separation of

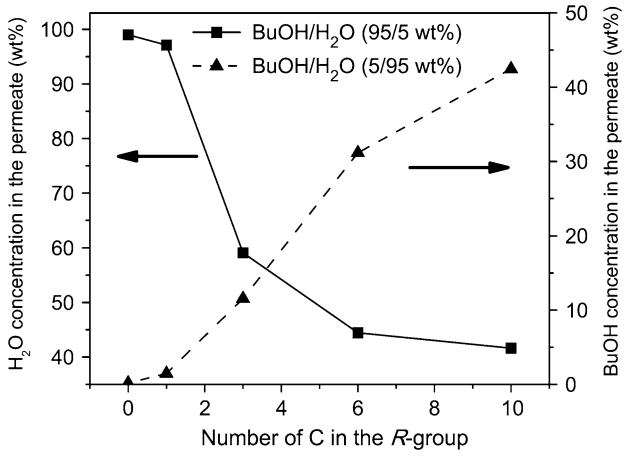

Fig. 7 Permeate concentration of BuOH and H_2O as function of the number of C atoms in the R group in pervaporation of *n*-butanol/water feed mixtures of 95/5 and 5/95 wt%. The feed concentrations were normalized to 5 wt% for direct comparison. Reprinted from Ref. [13] with permission from Elsevier

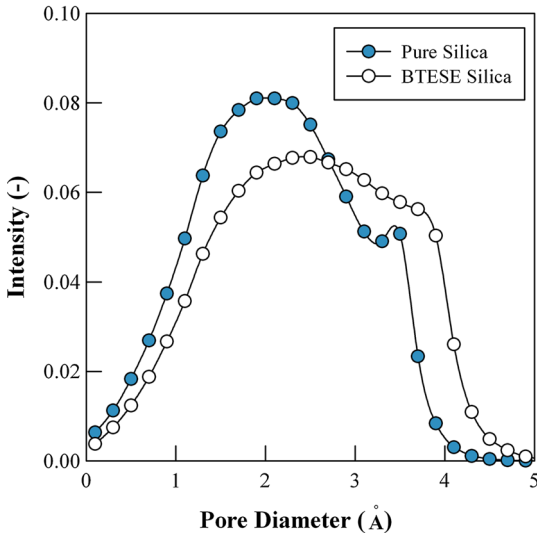

Fig. 8 Simulated cavity size distribution of the pure silica and hybrid BTESE silica membranes. Reproduced from Ref. [80] with permission from The Royal Society of Chemistry

larger molecules like propene (0.46 nm) from propane (0.50 nm) [82], see Fig. 9.

Apart from compositional differences, the sol–gel fabrication process itself also has a significant influence on the final properties of the membrane. Lower [Si] concentrations during the film coating process lead to more open pore structures and consequently to membranes with higher gas permeability [83]. Careful engineering of the pore structure via control over the conditions during membrane fabrication has been shown to lead to permselectivity increases of BTESE membranes to H_2/N_2 values of 50–400 [84]. Essentially, BTESE sols with a low acid ratio ($[H^+]/[Si] = 0.01$) that were coated onto supports that had been predried at very low relative humidity (RH < 1 %) yielded hybrid membranes with a considerably lower fraction of large pores > 0.35 nm than other membranes. The permeance of small gases (<0.35 nm) like He, H_2 and CO_2 was not affected, see Fig. 10. It is thought that the absence of a high concentration of protons in the sol [33] and the absence of excess water during condensation and film drying lead to a more densified silica film in which larger, non-selective pores are virtually absent.

Gas separations are usually carried out at elevated temperatures and pressures, and knowledge of the temperature and pressure dependency of the permeability of gases is therefore important. The temperature dependency of permeability of all molecules is typically positive or slightly negative, i.e., values for the activation energy between −1 and +2 kJ/mol are typical [12]. The only exception is CO_2 which tends to adsorb on the pore surface. The activation energy of permeability is the activation energy of diffusion minus the heat of sorption of the molecule on the inner pore wall [77], which is why its value can be either positive or negative. For CO_2, the activation energy is usually negative, since it adsorbs relatively strongly on micropore walls in silica and methylated silica, with corresponding heats of sorption that are larger than its activation energy of diffusion. Interestingly, the general trends observed in silica and methylated silica were also observed in hybrid organosilicas with varying alkylene and arylene bridges, irrespective of the type of gas and the type of bridge. The only exception was the $–C_8H_{16}–$ bridged membrane [12], which showed a relatively high activation energy of permeability of +6 kJ/mol for He, H_2, N_2 and CH_4 and +2 kJ/mol for CO_2. Since the end-to-end length of the organic bridge of the phenylene and di-phenylene bridges is similar, the difference must lie in the absence of rigidity of the chain. Apparently, the long and flexible $–C_8H_{16}–$ bridges have a retarding effect on the transport rate of all molecules, and this effect increases with temperature. Possibly the thermal vibration and conformational changes in the octylene bridge hinder gas transport. All other bridges are shorter or more rigid, and apparently that is beneficial for a high molecular transport rate.

In recent years, the separation of CO_2 from gas mixtures has been under serious consideration for sequestration purposes, but in general good membranes are lacking. The negative activation energy for CO_2 suggests that unlike other gases, its transport path is strongly influenced by chemical interactions with the hybrid organosilica matrix. Since its molecular size is larger than that of H_2, a CO_2

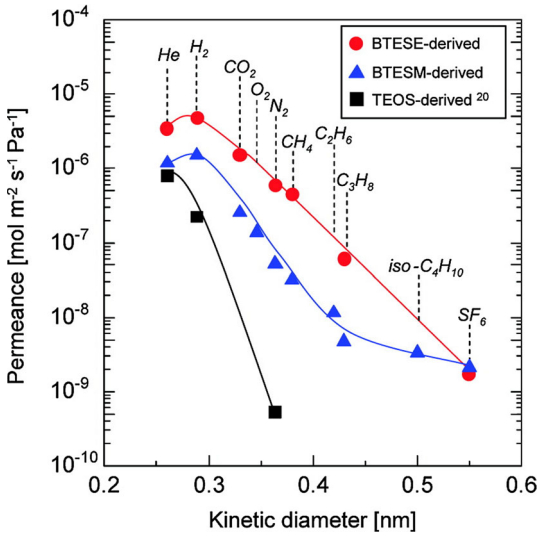

Fig. 9 Gas permeance versus molecular kinetic diameter of gases for BTESE, BTESM and inorganic silica membranes at 200 °C. Reprinted with permission from Ref. [41]. Copyright 2012 American Chemical Society

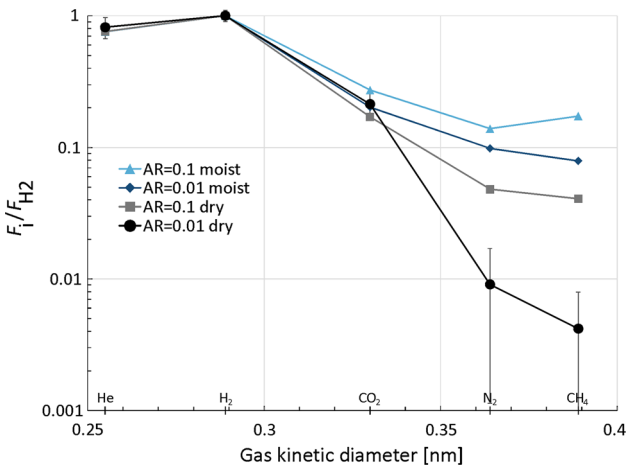

Fig. 10 Normalized single gas permeances of BTESE-based membranes prepared with acid ratio $[H^+]/[Si] = 0.01$ or 0.1, coated onto support systems pretreated at RH = 0.5 % ("dry") or 90 % ("moist"). Reference permeance is hydrogen flux at 473 K, $\Delta p = 2$ bar. Reprinted from Ref. [84] with permission from Elsevier

separation membrane operates ideally at low temperatures where adsorption of CO_2 is maximal. Moreover, in contrast to the other gases, the permeability of CO_2 decreases with increasing (average) pressure of the system, which is indicative of a strong influence of adsorption effects, see Fig. 11. Relatively high CO_2/H_2 permselectivities of 7–10 were obtained for ethylene and methylene-bridged membranes at 50 °C, but at 250 °C and 3 bar feed pressure the longer octylene, phenylene and di-phenylene bridged membranes performed better with values of 1.5–1.7. Apparently, the larger pore sizes in these membranes are beneficial for affinity-based transport at high temperature [12]. These studies show that the permeability of gases depends on the size, flexibility and nature of the organic bridging groups and that the selectivity of hybrid organosilica membranes can be tailored toward certain targeted molecules.

Inspired by an earlier study on the incorporation of Nb into a microporous silica membrane (Nb:Si = 1:3) to suppress the transport of CO_2 [20], Nb was also introduced into BTESE-derived silica [85, 86]. Just as with normal silica the diffusion of CO_2 was largely suppressed, leading to enhanced H_2/CO_2 permselectivity. Qi et al. explained these effects by the formation of acidic Nb sites in the matrix structure [20, 87], but also by possible densification effects due to the very high thermal annealing temperature for BTESE (400–550 °C in N_2) [86], temperatures at which thermal degradation of the organic bridges may have occurred [61, 86]. Other dopants that have been introduced into BTESE and BTESM matrices by co-condensation are aluminum (Al) [88], boron (B) and tantalum (Ta) [89]. In the latter study, a much lower thermal annealing temperature of 300 °C (in N_2) was employed. BTESE is known to be stable at this temperature even in air. In contrast to the work of Qi et al. [85, 86], no specific influence of the B, Ta or Nb dopants on CO_2 permeability was observed, apart from a general increase in membrane permeability for all gases, see Fig. 12. This suggests that densification effects due to thermal degradation of the ethylene bridge may have led to small enough pores for the Nb center to have an appreciable effect on CO_2 transport in the study of Qi, while the same sites did not influence CO_2 permselectivity in an intact BTESE-based matrix as in the study of Qureshi et al. [89] Recently, a malonamide-functional membrane with an ability to disperse transition metal ions homogeneously throughout the matrix was reported [17]. Both Ce^{4+} and Ni^{2+} were doped into the system. In both cases, enhanced H_2/N_2 selectivity was observed in comparison with the reference system BTESE. Particularly, the Ni-doped system showed considerable densification, so that all gas fluxes were ~10 times smaller than through the other membranes reported. Also recently, a triazine-functional hybrid organosilica membrane based on a novel sol–gel precursor was reported [18, 90]. The membrane had a high H_2/SF_6 selectivity and a high affinity for propene/propane separation.

4.3 Stability issues

BTESE membranes are resistant to aggressive aprotic solvents like *N*-methyl pyrrolidone (NMP), to organic acids like acetic acid [26, 91] and even to HNO_3 up to concentrations of 0.05 wt% in water–ethanol (pH 2.2) [26]. Only substantially higher concentrations of HNO_3 or the use of even stronger acids like methyl sulfonic acid led to fast deterioration of the membrane, leading to complete loss of performance within several days [26, 65]. Despite the fact that hybrid organosilica membranes are much more

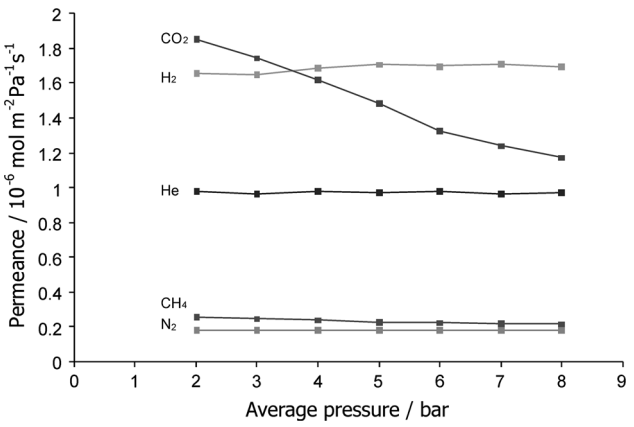

Fig. 11 Dependence of gas permeances on the average pressure with a constant pressure drop of 2 bar through a BTESM membrane at 50 °C. Reprinted from Ref. [12] with permission from Wiley

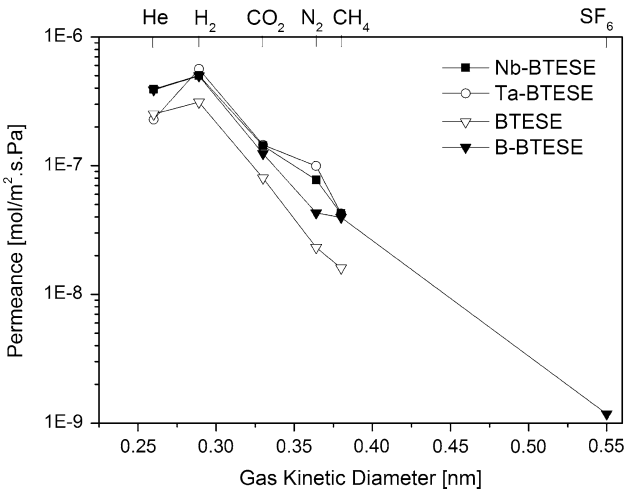

Fig. 12 Single gas permeances at 200 °C of undoped and Nb-, Ta- and B-doped BTESE sol–gel-derived membranes, annealed at 300 °C in N_2, as a function of kinetic diameter of permeating gases. Reprinted from Ref. [89]

resistant to high temperatures and hydrothermal conditions, they show some degree of performance loss over time. A slow degradation of the flux of 3–4 %/month at 150 °C was already reported in the first pervaporation studies [7, 19]. Similar performance was observed in a 1000-day test [28]; a water flux decline to approximately 50 % of its initial value was observed during the first 400 days of operation. The reason for this slow change is not understood. Since the separation factor in these studies remains high over this time period, the decreasing flux can be counteracted in practice by gradually increasing the operating temperature over the lifetime of the membrane, but there is obviously a limit to that option.

5 Conclusions

Microporous hybrid organosilica membranes have shown very good performance in industrially relevant gas and liquid separation processes. Control over membrane properties such as pore size and hydrophobicity via control of the nature of the bridging group has been demonstrated. However, the number of possible bridging groups is virtually infinite. Many other functional groups may be covalently incorporated into the hybrid organosilica matrix, thus giving rise to novel molecular sieving membranes with unexplored and possibly unprecedented separation performance. We expect to see new examples of membranes based on this principle in the forthcoming years. One of the still open questions in hybrid membrane engineering concerns the slow deterioration of the permeability of a membrane upon long-term exposure. While this did not hamper the introduction of hybrid organosilica membrane technology in industry, it does affect their lifetime and a better understanding of its molecular cause and possible cure are dearly needed.

References

1. Uhlhorn RJR, Keizer K, Burggraaf AJ (1992) Gas-transport and separation with ceramic membranes. II. Synthesis and separation properties of microporous membranes. J Membr Sci 66(2–3):271–287. doi:10.1016/0376-7388(92)87017-r
2. Delange RSA, Keizer K, Burggraaf AJ (1995) Analysis and theory of gas-transport in microporous sol–gel derived ceramic membranes. J Membr Sci 104(1–2):81–100. doi:10.1016/0376-7388(95)00014-4
3. van Veen HM, van Delft YC, Engelen CWR, Pex P (2001) Dewatering of organics by pervaporation with silica membranes. Sep Purif Technol 22–3(1–3):361–366. doi:10.1016/s1383-5866(00)00119-2
4. de Vos RM, Verweij H (1998) High-selectivity, high-flux silica membranes for gas separation. Science 279(5357):1710–1711. doi:10.1126/science.279.5357.1710
5. Asaeda M, Sakou Y, Yang JH, Shimasaki K (2002) Stability and performance of porous silica-zirconia composite membranes for pervaporation of aqueous organic solutions. J Membr Sci 209(1):163–175. doi:10.1016/s0376-7388(02)00327-7
6. Campaniello J, Engelen CWR, Haije WG, Pex P, Vente JF (2004) Long-term pervaporation performance of microporous methylated silica membranes. Chem Commun 7:834–835. doi:10.1039/b401496k
7. Castricum HL, Sah A, Kreiter R, Blank DHA, Vente JF, ten Elshof JE (2008) Hybrid ceramic nanosieves: stabilizing nanopores with organic links. Chem Commun 9:1103–1105. doi:10.1039/b718082a
8. Sekulic J, ten Elshof JE, Blank DHA (2004) A microporous titania membrane for nanofiltration and pervaporation. Adv Mater 16(17):1546–1550. doi:10.1002/adma.200306472
9. Lin YS, Kumakiri I, Nair BN, Alsyouri H (2002) Microporous inorganic membranes. Sep Purif Methods 31(2):229–379. doi:10.1081/spm-120017009
10. Lu GQ, da Costa JCD, Duke M, Giessler S, Socolow R, Williams RH, Kreutz T (2007) Inorganic membranes for hydrogen production and purification: a critical review and perspective. J Colloid Interface Sci 314(2):589–603. doi:10.1016/j.jcis.2007.05.067
11. Chapman PD, Oliveira T, Livingston AG, Li K (2008) Membranes for the dehydration of solvents by pervaporation. J Membr Sci 318(1–2):5–37. doi:10.1016/j.memsci.2008.02.061
12. Castricum HL, Paradis GG, Mittelmeijer-Hazeleger MC, Kreiter R, Vente JF, ten Elshof JE (2011) Tailoring the separation behavior of hybrid organosilica membranes by adjusting the structure of the organic bridging group. Adv Funct Mater 21(12):2319–2329. doi:10.1002/adfm.201002361
13. Paradis GG, Shanahan DP, Kreiter R, van Veen HM, Castricum HL, Nijmeijer A, Vente JF (2013) From hydrophilic to hydrophobic HybSi (R) membranes: a change of affinity and applicability. J Membr Sci 428:157–162. doi:10.1016/j.memsci.2012.10.006
14. Xu R, Ibrahim SM, Kanezashi M, Yoshioka T, Ito K, Ohshita J, Tsuru T (2014) New insights into the microstructure-separation properties of organosilica membranes with ethane, ethylene, and acetylene bridges. ACS Appl Mater Interfaces 6(12):9357–9364. doi:10.1021/am501731d
15. de Vos RM, Maier WF, Verweij H (1999) Hydrophobic silica membranes for gas separation. J Membr Sci 158(1–2):277–288. doi:10.1016/s0376-7388(99)00035-6
16. Paradis GG, Kreiter R, van Tuel MMA, Nijmeijer A, Vente JF (2012) Amino-functionalized microporous hybrid silica membranes. J Mater Chem 22(15):7258–7264. doi:10.1039/c2jm15417j
17. Besselink R, Qureshi HF, Winnubst L, ten Elshof JE (2015) A novel malonamide bridged silsesquioxane precursor for enhanced dispersion of transition metal ions in hybrid silica membranes. Microporous Mesoporous Mater 214:45–53
18. Ibrahim SM, Xu R, Nagasawa H, Naka A, Ohshita J, Yoshioka T, Kanezashi M, Tsuru T (2014) Insight into the pore tuning of triazine-based nitrogen-rich organoalkoxysilane membranes for use in water desalination. RSC Adv 4(45):23759–23769. doi:10.1039/c4ra02772h
19. Castricum HL, Sah A, Kreiter R, Blank DHA, Vente JF, ten Elshof JE (2008) Hydrothermally stable molecular separation membranes from organically linked silica. J Mater Chem 18(18):2150–2158. doi:10.1039/b801972j

20. Boffa V, ten Elshof JE, Petukhov AV, Blank DHA (2008) Microporous niobia-silica membrane with very low CO_2 permeability. ChemSusChem 1(5):437–443. doi:10.1002/cssc.200700165
21. Sekulic J, Magraso A, ten Elshof JE, Blank DHA (2004) Influence of ZrO_2 addition on microstructure and liquid permeability of mesoporous TiO_2 membranes. Microporous Mesoporous Mater 72(1–3):49–57. doi:10.1016/j.micromeso.2004.04.017
22. Loy DA, Carpenter JP, Alam TM, Shaltout R, Dorhout PK, Greaves J, Small JH, Shea KJ (1999) Cyclization phenomena in the sol–gel polymerization of alpha, omega-bis(triethoxysilyl) alkanes and incorporation of the cyclic structures into network silsesquioxane polymers. J Am Chem Soc 121(23):5413–5425. doi:10.1021/ja982751v
23. Yamamoto K, Ohshita J, Mizumo T, Tsuru T (2014) Polymerization behavior and gel properties of ethane, ethylene and acetylene-bridged polysilsesquioxanes. J Sol-Gel Sci Technol 71(1):24–30. doi:10.1007/s10971-014-3322-8
24. Castricum HL, Sah A, Geenevasen JAJ, Kreiter R, Blank DHA, Vente JF, ten Elshof JE (2008) Structure of hybrid organic–inorganic sols for the preparation of hydrothermally stable membranes. J Sol-Gel Sci Technol 48(1–2):11–17. doi:10.1007/s10971-008-1742-z
25. Kreiter R, Rietkerk MDA, Castricum HL, van Veen HM, ten Elshof JE, Vente JF (2009) Stable hybrid silica nanosieve membranes for the dehydration of lower alcohols. ChemSusChem 2(2):158–160. doi:10.1002/cssc.200800198
26. van Veen HM, Rietkerk MDA, Shanahan DP, van Tuel MMA, Kreiter R, Castricum HL, ten Elshof JE, Vente JF (2011) Pushing membrane stability boundaries with HybSi (R) pervaporation membranes. J Membr Sci 380(1–2):124–131. doi:10.1016/j.memsci.2011.06.040
27. Shea KJ, Loy DA (2001) A mechanistic investigation of gelation. The sol–gel polymerization of precursors to bridged polysilsesquioxanes. Acc Chem Res 34(9):707–716. doi:10.1021/ar000109b
28. Kreiter R, Rietkerk MDA, Castricum HL, van Veen HM, ten Elshof JE, Vente JF (2011) Evaluation of hybrid silica sols for stable microporous membranes using high-throughput screening. J Sol-Gel Sci Technol 57(3):245–252. doi:10.1007/s10971-010-2208-7
29. Glatter O, Kratky O (1982) Small angle X-ray scattering. Academic Press, London
30. Maene N, Nair BN, D'Hooghe P, Nakao SI, Keizer K (1998) Silica-polymers for processing gas separation membranes: high temperature growth of fractal structure. J Sol-Gel Sci Technol 12(2):117–134. doi:10.1023/a:1008617412933
31. Boffa V, Castricum HL, Garcia R, Schmuhl R, Petukhov AV, Blank DHA, ten Elshof JE (2009) Structure and growth of polymeric niobia-silica mixed-oxide sols for microporous molecular sieving membranes: a SAXS study. Chem Mat 21(9):1822–1828. doi:10.1021/cm802511w
32. Lin MY, Lindsay HM, Weitz DA, Ball RC, Klein R, Meakin P (1989) Universality in colloid aggregation. Nature 339(6223):360–362. doi:10.1038/339360a0
33. Castricum HL, Paradis GG, Mittelmeijer-Hazeleger MC, Bras W, Eeckhaut G, Vente JF, Rothenberg G, ten Elshof JE (2014) Tuning the nanopore structure and separation behavior of hybrid organosilica membranes. Microporous Mesoporous Mater 185:224–234. doi:10.1016/j.micromeso.2013.11.005
34. Besselink R, Stawski TM, Castricum HL, ten Elshof JE (2013) Evolution of microstructure in mixed niobia-hybrid silica thin films from sol–gel precursors. J Colloid Interface Sci 404:24–35. doi:10.1016/j.jcis.2013.04.031
35. Besselink R, ten Elshof JE (2014) Mass-fractal growth in niobia/silsesquioxane mixtures: a small-angle X-ray scattering study. J Appl Crystallogr 47:1606–1613. doi:10.1107/s1600576714017105
36. Besselink R, Venkatachalam S, van Wullen L, ten Elshof J (2014) Incorporation of niobium into bridged silsesquioxane based silica networks. J Sol-Gel Sci Technol 70(3):473–481. doi:10.1007/s10971-014-3308-6
37. Lee HR, Kanezashi M, Yoshioka T, Tsuru T (2010) Preparation of hydrogen separation membranes using disiloxane compounds. Desalin Water Treat 17(1–3):120–126. doi:10.5004/dwt.2010.1707
38. Lee HR, Kanezashi M, Shimomura Y, Yoshioka T, Tsuru T (2011) Evaluation and fabrication of pore-size-tuned silica membranes with tetraethoxydimethyl Disiloxane for gas separation. AIChE J 57(10):2755–2765. doi:10.1002/aic.12501
39. Li G, Kanezashi M, Tsuru T (2011) Preparation of organic–inorganic hybrid silica membranes using organoalkoxysilanes: the effect of pendant groups. J Membr Sci 379(1–2):287–295. doi:10.1016/j.memsci.2011.05.071
40. Ma Y, Lee HR, Okahana K, Kanezashi M, Yoshioka T, Tsuru T (2013) Preparation and characterization of methyl-modified hybrid silica membranes for gas separation. Desalin Water Treat 51(25–27):5149–5154. doi:10.1080/19443994.2013.768409
41. Kanezashi M, Kawano M, Yoshioka T, Tsuru T (2012) Organic–inorganic hybrid silica membranes with controlled silica network size for propylene/propane separation. Ind Eng Chem Res 51(2):944–953. doi:10.1021/ie201606k
42. Kanezashi M, Yada K, Yoshioka T, Tsuru T (2010) Organic–inorganic hybrid silica membranes with controlled silica network size: preparation and gas permeation characteristics. J Membr Sci 348(1–2):310–318. doi:10.1016/j.memsci.2009.11.014
43. Kappert EJ, Bouwmeester HJM, Benes NE, Nijmeijer A (2014) Kinetic analysis of the thermal processing of silica and organosilica. J Phys Chem B 118(19):5270–5277. doi:10.1021/jp502344k
44. Hunks WJ, Ozin GA (2005) Engineering porosity in bifunctional periodic mesoporous organosilicas with MT- and DT-type silica building blocks. J Mater Chem 15(7):764–771. doi:10.1039/b412963f
45. Hunks WJ, Ozin GA (2005) Single-source precursors for synthesizing bifunctional periodic mesoporous organosilicas. Adv Funct Mater 15(2):259–266. doi:10.1002/adfm.200400294
46. Small JH, Shea KJ, Loy DA (1993) Arylene-bridged and alkylene-bridged polysilsesquioxanes. J Non-Cryst Solids 160(3):234–246. doi:10.1016/0022-3093(93)91267-7
47. Wang W, Grozea D, Kohli S, Perovic DD, Ozin GA (2011) Water repellent periodic mesoporous organosilicas. ACS Nano 5(2):1267–1275. doi:10.1021/nn102929t
48. Goethals F, Vercaemst C, Cloet V, Hoste S, Van Der Voort P, Van Driessche I (2010) Comparative study of ethylene- and ethenylene-bridged periodic mesoporous organosilicas. Microporous Mesoporous Mater 131(1–3):68–74. doi:10.1016/j.micromeso.2009.12.004
49. Guo WP, Li X, Zhao XS (2006) Understanding the hydrothermal stability of large-pore periodic mesoporous organosilicas and pure silicas. Microporous Mesoporous Mater 93(1–3):285–293. doi:10.1016/j.micromeso.2006.03.009
50. Kanezashi M, Yada K, Yoshioka T, Tsuru T (2009) Design of silica networks for development of highly permeable hydrogen separation membranes with hydrothermal stability. J Am Chem Soc 131(2):414–415. doi:10.1021/ja806762q
51. Wahab MA, He CB (2011) Hydrothermally stable periodic mesoporous ethane-silica and bimodal mesoporous nanostructures. J Nanosci Nanotechnol 11(10):8481–8487. doi:10.1166/jnn.2011.4962
52. Tsuru T, Nakasuji T, Oka M, Kanezashi M, Yoshioka T (2011) Preparation of hydrophobic nanoporous methylated SiO_2 membranes and application to nanofiltration of hexane solutions. J Membr Sci 384(1–2):149–156. doi:10.1016/j.memsci.2011.09.018

53. Cerveau G, Corriu RJP, Dabosi J, Aubagnac JL, Combarieu R, de Puydt Y (1998) TOF-SIMS characterization of the surface of monophase hybrid organic inorganic materials. J Mater Chem 8(8):1761–1767. doi:10.1039/a802003e
54. Rao AV, Latthe SS, Nadargi DY, Hirashima H, Ganesan V (2009) Preparation of MTMS based transparent superhydrophobic silica films by sol–gel method. J Colloid Interface Sci 332(2):484–490. doi:10.1016/j.jcis.2009.01.012
55. Latthe SS, Imai H, Ganesan V, Rao AV (2010) Ultrahydrophobic silica films by sol–gel process. J Porous Mat 17(5):565–571. doi:10.1007/s10934-009-9325-0
56. Latthe SS, Nadargi DY, Rao AV (2009) TMOS based water repellent silica thin films by co-precursor method using TMES as a hydrophobic agent. Appl Surf Sci 255(6):3600–3604. doi:10.1016/j.apsusc.2008.10.005
57. Latthe SS, Imai H, Ganesan V, Rao AV (2010) Porous superhydrophobic silica films by sol–gel process. Microporous Mesoporous Mater 130(1–3):115–121. doi:10.1016/j.micromeso.2009.10.020
58. Latthe SS, Imai H, Ganesan V, Kappenstein C, Rao AV (2010) Optically transparent superhydrophobic TEOS-derived silica films by surface silylation method. J Sol-Gel Sci Technol 53(2):208–215. doi:10.1007/s10971-009-2079-y
59. Rao AV, Latthe SS, Mahadik SA, Kappenstein C (2011) Mechanically stable and corrosion resistant superhydrophobic sol–gel coatings on copper substrate. Appl Surf Sci 257(13):5772–5776. doi:10.1016/j.apsusc.2011.01.099
60. Shateri-Khalilabad M, Yazdanshenas ME (2013) One-pot sonochemical synthesis of superhydrophobic organic–inorganic hybrid coatings on cotton cellulose. Cellulose 20(6):3039–3051. doi:10.1007/s10570-013-0040-2
61. Agirre I, Arias PL, Castricum HL, Creatore M, ten Elshof JE, Paradis GG, Ngamou PHT, van Veen HM, Vente JF (2014) Hybrid organosilica membranes and processes: status and outlook. Sep Purif Technol 121:2–12. doi:10.1016/j.seppur.2013.08.003
62. Cerveau G, Corriu RJP, Lepeytre C, Mutin PH (1998) Influence of the nature of the organic precursor on the textural and chemical properties of silsesquioxane materials. J Mater Chem 8(12):2707–2713. doi:10.1039/a805794j
63. Cerveau G, Corriu RJP, Dabosi J, Fischmeister-Lepeytre C, Combarieu R (1999) Characterization of the surface organization of nanostructured hybrid organic–inorganic materials by time-of-flight secondary ion mass spectrometry. Rapid Commun Mass Spectrom 13(21):2183–2190. doi:10.1002/(sici)1097-0231(19991115)13:21<2183:aid-rcm773>3.3.co;2-7
64. Shimoyama T, Yoshioka T, Nagasawa H, Kanezashi M, Tsuru T (2013) Molecular dynamics simulation study on characterization of bis(triethoxysilyl)-ethane and bis(triethoxysilyl)ethylene derived silica-based membranes. Desalin Water Treat 51(25–27):5248–5253. doi:10.1080/19443994.2013.768747
65. Castricum HL, Kreiter R, van Veen HM, Blank DHA, Vente JF, ten Elshof JE (2008) High-performance hybrid pervaporation membranes with superior hydrothermal and acid stability. J Membr Sci 324(1–2):111–118. doi:10.1016/j.memsci.2008.07.014
66. Li DF, Han Y, Song HW, Zhao L, Xu XZ, Di Y, Xiao FS (2004) High-temperature synthesis of stable ordered mesoporous silica materials by using fluorocarbon–hydrocarbon surfactant mixtures. Chem-Eur J 10(23):5911–5922. doi:10.1002/chem.200400188
67. Kappert EJ, Pavlenko D, Malzbender J, Nijmeijer A, Benes NE, Tsai PA (2015) Formation and prevention of fractures in sol–gel-derived thin films. Soft Matter 11(5):882–888. doi:10.1039/c4sm02085e
68. Dubois G, Volksen W, Magbitang T, Miller RD, Gage DM, Dauskardt RH (2007) Molecular network reinforcement of sol–gel glasses. Adv Mater 19(22):3989. doi:10.1002/adma.200701193
69. Oliver MS, Dubois G, Sherwood M, Gage DM, Dauskardt RH (2010) Molecular origins of the mechanical behavior of hybrid glasses. Adv Funct Mater 20(17):2884–2892. doi:10.1002/adfm.201000558
70. Pauling L (1960) The nature of the chemical bond and the structure of molecules and crystals—an introduction to modern structural chemistry, 3rd edn. Oxford University Press, London
71. Pauling L (1980) The nature of silicon–oxygen bonds. Am Miner 65(3–4):321–323
72. Bromley ST, Bandow B, Hartke B (2008) Structural correspondences between the low-energy nanoclusters of silica and water. J Phys Chem C 112(47):18417–18425. doi:10.1021/jp806780w
73. Angell CA, Kanno H (1976) Density maxima in high-pressure supercooled water and liquid silicon dioxide. Science 193(4258):1121–1122. doi:10.1126/science.193.4258.1121
74. Tsuneyuki S, Matsui Y (1995) Molecular-dynamics study of pressure enhancement of ion mobilities in liquid silica. Phys Rev Lett 74(16):3197–3200. doi:10.1103/PhysRevLett.74.3197
75. Wragg DS, Morris RE, Burton AW (2008) Pure silica zeolite-type frameworks: a structural analysis. Chem Mat 20(4):1561–1570. doi:10.1021/cm071824j
76. Nair BN, Keizer K, Suematsu H, Suma Y, Kaneko N, Ono S, Okubo T, Nakao SI (2000) Synthesis of gas and vapor molecular sieving silica membranes and analysis of pore size and connectivity. Langmuir 16(10):4558–4562. doi:10.1021/la9906471
77. ten Elshof JE, Abadal CR, Sekulic J, Chowdhury SR, Blank DHA (2003) Transport mechanisms of water and organic solvents through microporous silica in the pervaporation of binary liquids. Microporous Mesoporous Mater 65(2–3):197–208. doi:10.1016/j.micromeso.2003.08.010
78. Gallego-Lizon T, Edwards E, Lobiundo G, dos Santos LF (2002) Dehydration of water/t-butanol mixtures by pervaporation: comparative study of commercially available polymeric, microporous silica and zeolite membranes. J Membr Sci 197(1–2):309–319. doi:10.1016/s0376-7388(01)00650-0
79. Sekulic J, Luiten MWJ, ten Elshof JE, Benes NE, Keizer K (2002) Microporous silica and doped silica membrane for alcohol dehydration by pervaporation. Desalination 148(1–3):19–23. doi:10.1016/s0011-9164(02)00647-1
80. Chang KS, Yoshioka T, Kanezashi M, Tsuru T, Tung KL (2010) A molecular dynamics simulation of a homogeneous organic–inorganic hybrid silica membrane. Chem Commun 46(48):9140–9142. doi:10.1039/c0cc02531c
81. Chang KS, Yoshioka T, Kanezashi M, Tsuru T, Tung KL (2011) Molecular simulation of micro-structures and gas diffusion behavior of organic–inorganic hybrid amorphous silica membranes. J Membr Sci 381(1–2):90–101. doi:10.1016/j.memsci.2011.07.020
82. Kanezashi M, Shazwani WN, Yoshioka T, Tsuru T (2012) Separation of propylene/propane binary mixtures by bis(triethoxysilyl) methane (BTESM)-derived silica membranes fabricated at different calcination temperatures. J Membr Sci 415:478–485. doi:10.1016/j.memsci.2012.05.034
83. Qureshi HF, Nijmeijer A, Winnubst L (2013) Influence of sol–gel process parameters on the micro-structure and performance of hybrid silica membranes. J Membr Sci 446:19–25. doi:10.1016/j.memsci.2013.06.024
84. Castricum HL, Qureshi HF, Nijmeijer A, Winnubst L (2015) Hybrid silica membranes with enhanced hydrogen and CO_2 separation properties. J Membr Sci 488:121–128. doi:10.1016/j.memsci.2015.03.084

85. Qi H, Han J, Xu NP, Bouwmeester HJM (2010) Hybrid organic–inorganic microporous membranes with high hydrothermal stability for the separation of carbon dioxide. ChemSusChem 3(12):1375–1378. doi:10.1002/cssc.201000242
86. Qi H, Chen HR, Li L, Zhu GZ, Xu NP (2012) Effect of Nb content on hydrothermal stability of a novel ethylene-bridged silsesquioxane molecular sieving membrane for H_2^-/CO_2 separation. J Membr Sci 421:190–200. doi:10.1016/j.memsci.2012.07.010
87. Boffa V, ten Elshof JE, Garcia R, Blank DHA (2009) Microporous niobia-silica membranes: influence of sol composition and structure on gas transport properties. Microporous Mesoporous Mater 118(1–3):202–209. doi:10.1016/j.micromeso.2008.08.038
88. Kanezashi M, Miyauchi S, Nagasawa H, Yoshioka T, Tsuru T (2013) Pore size control of Al-doping into bis (triethoxysilyl) methane (BTESM)-derived membranes for improved gas permeation properties. RSC Adv 3(30):12080–12083. doi:10.1039/c3ra41971a
89. Qureshi HF, Besselink R, ten Elshof JE, Nijmeijer A, Winnubst L (2015) Doped microporous hybrid silica membranes for gas separation. J Sol-Gel Sci Technol 75(1):180–188. doi:10.1007/s10971-015-3687-3
90. Ibrahim SM, Xu R, Nagasawa H, Naka A, Ohshita J, Yoshioka T, Kanezashi M, Tsuru T (2014) A closer look at the development and performance of organic–inorganic membranes using 2,4,6-tris-3(triethoxysilyl)-1-propoxyl-1,3,5-triazine (TTESPT). RSC Adv 4(24):12404–12407. doi:10.1039/c3ra47736c
91. Tsuru T, Shibata T, Wang JH, Lee HR, Kanezashi M, Yoshioka T (2012) Pervaporation of acetic acid aqueous solutions by organosilica membranes. J Membr Sci 421:25–31. doi:10.1016/j.memsci.2012.06.012